Study and parameter identification of a model coupling cell signaling and gene expression

I. Ndiaye, M. Chaves and J.-L. Gouzé

***Abstract*— A schematic model composed of a basic signal transduction unit and one gene is presented. The regulation of the signaling pathway by gene expression patterns is analyzed. In particular, it is shown that a slowly varying gene expression pattern can induce rapid changes in the steady states or modes of operation of the (normally varying) signal transduction pathways, and lead to sustained oscillations. As an application, a system which operates during the G2 to M phase progression in embryonic cell cycle (the activation of cell division cycle protein Cdc2 by cyclin B) is analyzed, and some parameters identified.**

I. INTRODUCTION

Signaling pathways and gene expression can be viewed as two fundamental levels of intercellular organization and regulation. The former are responsible for transmitting information from the exterior to the interior of the cell (or between two intercellular regions), along signal transduction cascades. Gene transcription is often the ultimate result of signaling events but, conversely, changes in gene expression patterns can also activate a signal transduction cascade. Signaling pathways and genetic networks frequently interact to regulate cellular functions, in response to external stimuli. In general, signal transduction pathways and gene networks operate at different timescales. Typical signaling times are on the order of seconds, a fast process when compared to gene expression patterning (which may range from minutes to days). In this paper, we will focus on studying the interaction between fast and slower processes, such as signaling and genetic networks, or two signaling networks operating at different timescales. Examples of signaling pathways include the widely studied mitogen activated protein kinase (MAPK) cascades, consisting of a family of proteins which are activated sequentially. Several mathematical models have been proposed for MAPK cascades [5], [3], [1], [2].

To study the interaction between fast (eg., signaling) and slow (eg., genetic) networks, a simple loop with one gene product is coupled to the signal transduction unit proposed in [2]. It is assumed that protein x in this model activates transcription of a gene y, and that the corresponding protein Y promotes degradation of x (see Fig. 1). In this context, the present work proposes a mechanism for regulation of the dynamics of the signaling network by slowly varying dynamical patterns. In particular, if the signal transduction network has multiple steady states (representing different modes of operation), the role of the slow (eg., genetic) network in inducing major changes, or possible oscillations, in the concentrations of signaling proteins will be analyzed.

Corresponding author: M. Chaves. The authors are with COMORE, INRIA, 2004 Route des Lucioles, BP 93, 06902 Sophia Antipolis, France. Emails: {indiaye,mchaves,gouze}@sophia.inria.fr

Examples of biological systems where signaling pathways and genetic networks interact in this way include the $p53$-Mdm2 system [6] and the IκB - NFκB pathway [4] nuclear factor κB activates transcription of its own inhibitor (IκB mRNA), leading to oscillatory behavior [9]. Another biological system which appears to operate according to a similar fast/slow dynamical mechanism is the activation of Cdc2 (a cell division cycle protein) by cyclin B, during the progression from G2 to M phases in the early embryonic cell cycle in *Xenopus laevis* oocytes [11], [10]. Cyclin B (represented by Φ_0 in Fig. 1) activates Cdc2 (x_0), to form a complex Cdc2-cyclin B (x). This complex activates its own activator Cdc25 (represented by the '$+$' loop), and at the same time Cdc2 activates the Anaphase Promoting Complex (Y), which in turn promotes degradation of cyclin B (inactivation of x back to form x_0).

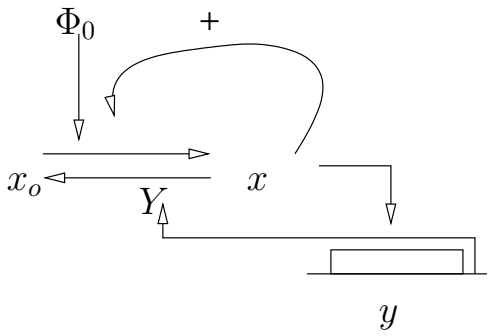

Fig. 1. Simplified scheme of the mechanism of regulation.

In [11] several experiments are reported, showing that the Cdc2-cyclin B system does exhibit two stable modes of operation. Available measurements include Cdc2-cyclin B steady state curves in response to constant input values of cyclin B. Further experiments by the same authors in [10] show that the auto-activation positive feedback (denoted '$+$' in Fig. 1) is necessary for sustained oscillations to occur. The present work focuses instead on the role of the slowly varying negative feedback loop (formed by the network y, Y). Using steady state data from [11], some of the model's parameters are identified. Our analysis provides some conditions for the existence of oscillations, as well as some predictions on the period of oscillations and its dependence on the model's parameters.

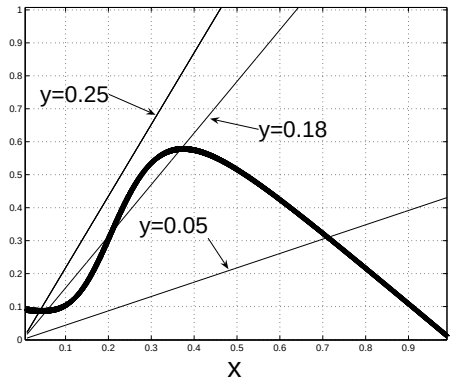

Fig. 2. The bold curve represents $\Phi(x) = (\Phi_0 + V_1 \frac{x^n}{x^n+\theta_1^n})(X_{tot} - x)$ and the other curves represent $\psi = \gamma_1 yx$ for three values of y. Values of parameters: $\Phi_0 = 0.09$, $X_{tot} = V_1 = 1$, $V_2 = 1.275 \times 10^{-2}$, $\gamma_1 = 8.7$, $\gamma_2 = 3.75 \times 10^{-2}$, $\theta_1 = 0.25$, $\theta_2 = 0.2$, $n = 4$, $m = 50$.

II. The model

In this model, a signal transduction unit consisting of two proteins x (active form) and x_0 (inactive form) is coupled to a simple genetic network, consisting of one messenger RNA and its corresponding protein (see Fig. 1). For simplicity, the genetic network will be represented by one variable only, y. An external signal or input (Φ_0) activates transformation of protein x_0 to its form x. An auto-activation feedback loop (represented by a term of the form $V_1 \frac{x^n}{x^n+\theta_1^n} x_0$), further promotes production of x. Activation of transcription by protein x is represented by the term $V_2 \frac{x^m}{x^m+\theta_2^m}$ and regulation of the degradation of protein x by the genetic network is represented by $-\gamma_1 yx$. γ_2 is the degradation rate of gene y. Taking the total concentration of protein to be constant, $x_0 + x = X_{tot}$, the equations are given by:

$$\begin{aligned} \dot{x} &= \Phi(x) - \gamma_1 yx = f(x,y) \\ \dot{y} &= V_2 \frac{x^m}{x^m + \theta_2^m} - \gamma_2 y = g(x,y) \end{aligned} \qquad (1)$$

where

$$\Phi(x) = \left(\Phi_0 + V_1 \frac{x^n}{\theta_1^n + x^n}\right)(X_{tot} - x).$$

All parameters are positive, and it is easy to see that the non-negative orthant ($[0,\infty[\times[0,\infty[$) is invariant for the system. The x equation follows closely one of the signaling modules analyzed in [2]: the new feature is that the degradation rate is now regulated by gene product y.

For each fixed $y > 0$, the steady states of x are obtained by solving the equation (for $x < X_{tot}$): $\Phi(x) = \gamma_1 yx$. As shown in [8], there are at least one (see Fig. 2, cases $y = 0.01$ or $y = 0.1$) and at most three (see Fig. 2, case $y = 0.05$) steady states for system (1). In this paper, we will consider the case when multiple steady states for x exist, representing different modes of operation of the signal transduction network (for each fixed y, in an appropriate interval). Next, letting y vary according to (1), we will study the response of x under the hypothesis that there is a significant difference between the timescales of dynamical processes governing x and y. Our goal is to study the role of slow processes (such as a genetic network) in the regulation of a faster process (such as a signal transduction network). In particular, we will study conditions under which the slower dynamics can induce the fast signaling network to jump between two steady states, or modes of operation.

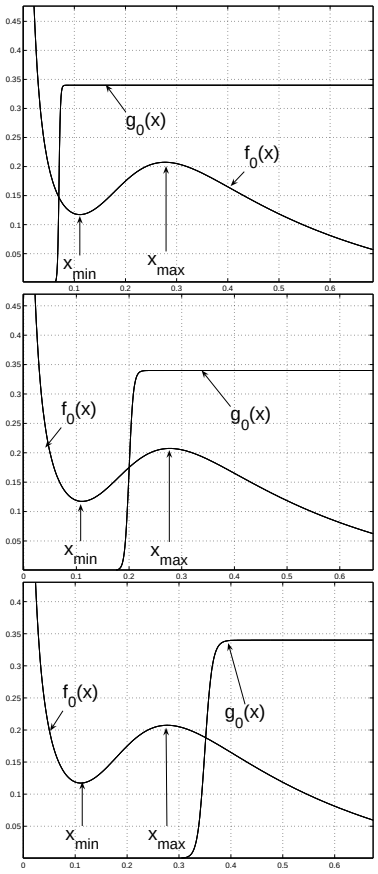

Fig. 3. Representation of nullclines. By varying θ_2, one of two cases is obtained: either θ_2 belongs to the interval $]x_{\min}, x_{\max}[$ (middle figure); or θ_2 is outside the interval $[x_{\min}, x_{\max}]$, either below $x_{\min}$ (top figure), or above $x_{\max}$ (bottom figure). Parameters are as in Fig. 2 and (top to bottom) a) $\theta_2 = 0.07$, b) $\theta_2 = 0.2$, and c) $\theta_2 = 0.35$.

III. Analysis of stability

To study the dynamics of system (1), we will first state suitable hypotheses (A1-A6 below) and characterize the steady states of the system. The nullclines of system (1) are defined by the equations $f(x,y) = 0$ and $g(x,y) = 0$, which can be solved for y to obtain:

$$f_0(x) = \frac{(\Phi_0 + V_1 \frac{x^n}{x^n+\theta_1^n})(X_{tot} - x)}{\gamma_1 x},$$

$$g_0(x) = \frac{V_2}{\gamma_2} \frac{x^m}{x^m + \theta_2^m}.$$

Here, we will study the system under the following assumptions on the parameters:

A1. $\gamma_2 < \min\{1, \frac{1}{2}X_{tot}, \frac{X_{tot}\Phi_0}{\Phi_0+V_2}\}$ and $\gamma_2 \ll \frac{\gamma_1}{\gamma_2}V_2$;

A2. m is large;

A3. there exist $0 < x_{\min} < x_{\max}$ with $df_0/dx(x_{\min}) = df_0/dx(x_{\max}) = 0$, $df_0/dx > 0$ for all $x \in]x_{\min}, x_{\max}[$, and $df_0/dx < 0$ for all $x \notin [x_{\min}, x_{\max}]$;

A4. $f_0(x_{\max}) < \max(g_0)$ (or $f_0(x_{\max}) < \frac{V_2}{\gamma_2}$, when m tends to infinity);

A5. $f_0(x_{\min}) > \min(g_0)$ (or $f_0(x_{\max}) > 0$, when m tends to infinity); and

A6. $n > \frac{1+\alpha^n}{1-\alpha\theta_1/X_{tot}} \left(\frac{\Phi_0}{V_1} \frac{1+\alpha^n}{\alpha^n} + 1 \right)$, for any $\alpha \in [1/2, 1]$.

Assumption A3 implies that f_0 increases in $]x_{\min}, x_{\max}[$ and decreases in $[0, x_{\min}]$ and $[x_{\max}, X_{tot}]$ (see Fig. 3). Below (Lemma 4.1, with assumption A6) explicit conditions on the parameters are given for A3. Assumptions A2, A4 and A5 imply that f_0 and g_0 intersect in a single point (x^*, y^*), as seen in Fig. 3. Stability of this intersection point will be analyzed for two cases: a) $\theta_2 \notin [x_{\min}, x_{\max}]$, and b) $\theta_2 \in]x_{\min}, x_{\max}[$. (The analysis of the particular cases $\theta_2 = x_{\min}$ or $\theta_2 = x_{\max}$ will not be presented here.) We deduce the following relations from the equation of nullclines,

$$\frac{\partial f(x,y)}{\partial x} + \frac{\partial f(x,y)}{\partial y}\Big(\frac{dy}{dx}\Big)_1 = 0$$
$$\frac{\partial g(x,y)}{\partial x} + \frac{\partial g(x,y)}{\partial y}\Big(\frac{dy}{dx}\Big)_2 = 0. \qquad (2)$$

Let $s_1 = \left(\frac{dy}{dx}\right)_1$ and $s_2 = \left(\frac{dy}{dx}\right)_2$ be, respectively, the slopes of nullclines $f(x,y) = 0$ and $g(x,y) = 0$ at steady state (x^*, y^*). The Jacobian is given by

$$J = \begin{bmatrix} \partial f/\partial x & \partial f/\partial y \\ \partial g/\partial x & \partial g/\partial y \end{bmatrix} = \begin{bmatrix} -s_1 \partial f/\partial y & \partial f/\partial y \\ -s_2 \partial g/\partial y & \partial g/\partial y \end{bmatrix}.$$

We know that, for a system of second order, the steady state is stable if the trace $\mathrm{tr}J < 0$ and the determinant $\det J > 0$. The steady state is unstable if $\mathrm{tr}J > 0$ and $\det J > 0$. General conditions for stability are:

C_1: $s_1 < \dfrac{\partial g(x,y)}{\partial y}\Big|_{(x^*,y^*)} \left(\dfrac{\partial f(x,y)}{\partial y}\Big|_{(x^*,y^*)} \right)^{-1}$

C_2 : $s_2 > s_1$,

where C_1 implies $\mathrm{tr}J < 0$ and C_2 implies $\det J > 0$. For parameter sets satisfying A1-A5, condition C_2 is always satisfied: indeed, for $\theta_2 \notin [x_{\min}, x_{\max}]$, $s_1 < 0 < s_2$, and for $\theta_2 \in]x_{\min}, x_{\max}[$ it can be seen directly from Fig. 3 that $s_2 > s_1$. Condition C_1 is satisfied if $\theta_2 \notin [x_{\min}, x_{\max}]$: note that $\mathrm{tr}J = -s_1 \partial f/\partial y + \partial g/\partial y = s_1\gamma_1 x^* - \gamma_2 < 0$, since $s_1 < 0$. So case a) always yields a stable steady state.

The next lemma characterizes case b), which admits an unstable steady state (see also Fig. 4).

Lemma 3.1: Assume A1-A5 hold. If $\theta_2 \in]x_{\min}, x_{\max}[$, then system (1) admits a stable limit cycle.

Proof. Let $\theta_2 \in]x_{\min}, x_{\max}[$ and prove, first, that the unique steady state (x^*, y^*) is unstable. It was shown above that $\det J > 0$. To show that $\mathrm{tr}J = s_1\gamma_1 x^* - \gamma_2 > 0$, note that $s_1 > 0$ and that $x^* > x_{\min}$. Note also that $x_{\min}$ is independent of γ_2 (since obtained from $df_0/dx = 0$). Thus, using assumption A1, one can choose γ_2 sufficently small such that $\gamma_2 < s_1\gamma_1 x_{\min} < s_1\gamma_1 x^*$.

To prove the existence of a stable limit cycle, the theorem of Poincaré-Bendixon can be applied. First, we will show that the set $\mathcal{D} = [\gamma_2, X_{tot}] \times [\frac{V_2}{2}\frac{\gamma_2^{m-1}}{\gamma_2^m + \theta_2^m}, V_2/\gamma_2]$ is an invariant compact set which contains the unstable point (x^*, y^*). To determine whether a given domain $\mathcal{D}$ is invariant, we evaluate the vector field on the boundary of the domain. If the vector field points towards the interior of $\mathcal{D}$, then $\mathcal{D}$ is invariant. It is clear that $\frac{dx}{dt} < 0$ whenever $x = X_{tot}$, and $\frac{dy}{dt} \leq 0$ whenever $y = \frac{V_2}{\gamma_2}$. Using assumption A1, one can choose γ_2 sufficiently small such that $\frac{dx}{dt} > 0$ when $x = \gamma_2$, and $\frac{dy}{dt} > 0$ when $y = \frac{V_2}{2}\frac{\gamma_2^{m-1}}{\gamma_2^m + \theta_2^m}$. Hence, the domain $\mathcal{D}$ is invariant and contains an unique unstable steady state. We deduce that $\mathcal{D}$ contains a stable limit cycle. ∎

IV. Fast and slow dynamics

In this section, we will give sufficient conditions for the system to exhibit a limit cycle, and then estimate its period in terms of the parameters. Lemma 3.1 shows that one needs to choose θ_2 in the interval $]x_{\min}, x_{\max}[$. But it is not easy to find explicit expressions for $x_{\min}$ and $x_{\max}$ in terms of the parameters of the system. To solve this problem, we will instead show that there exists $\Delta > 0$ such that the interval $I = [(1-\Delta)\theta_1, \theta_1] \subset]x_{\min}, x_{\max}[$. In this case, a sufficient condition for existence of an unstable equilibrium point is $\theta_2 \in [(1-\Delta)\theta_1, \theta_1]$.

Following the biologically reasonable assumption that the dynamics of the signaling network is faster than the dynamics of the genetic network, we can rewrite the model under a standard slow/fast approach (under a fast time): $\dot{x} = f(x,y)$ and $\dot{y} = \gamma_2 g(x,y)$ with γ_2 small (see A1). Normalizing variables and parameters to:

$$\widetilde{x} = \frac{x}{X_{tot}}, \quad \widetilde{y} = \gamma_2 \frac{y}{V_2}, \quad \tilde{\theta}_1 = \frac{\theta_1}{X_{tot}}, \quad \tilde{\theta}_2 = \frac{\theta_2}{X_{tot}},$$

system (1) can be rewritten as:

$$\frac{d\widetilde{x}}{dt} = \Big(\Phi_0 + V_1 \frac{\widetilde{x}^n}{\widetilde{x}^n + \tilde{\theta}_1^n}\Big)(1 - \widetilde{x}) - \gamma_1 \frac{V_2}{\gamma_2}\widetilde{y}\widetilde{x}$$
$$\frac{d\widetilde{y}}{dt} = \gamma_2 \left(\frac{\widetilde{x}^m}{\widetilde{x}^m + \tilde{\theta}_2^m} - \widetilde{y} \right) \qquad (3)$$

where $\frac{\gamma_1}{\gamma_2} V_2 \gg \gamma_2$ (see A1). In these new variables, Lemma 3.1 applies with $\tilde{\theta}_2$, $\widetilde{x}_{\max} = x_{\max}/X_{tot}$, and $\widetilde{x}_{\min} = x_{\min}/X_{tot}$. The new x-nullcline is given by $\tilde{f}_0(\widetilde{x}) = (\Phi_0 + V_1 \frac{\widetilde{x}^n}{\widetilde{x}^n + \tilde{\theta}_1^n}) \frac{1-\widetilde{x}}{\widetilde{x}} \frac{\gamma_2}{\gamma_1 V_2}$. The next Lemma gives explicit estimates for the local extrema of $\tilde{f}_0$, $\widetilde{x}_{\min}$ and $\widetilde{x}_{\max}$ (see assumption A3):

Lemma 4.1: Suppose assumption A6 holds. Then $\widetilde{x}_{\min} < \alpha\tilde{\theta}_1$ and $\widetilde{x}_{\max} > \tilde{\theta}_1$. ∎

To prove this Lemma, it is sufficient to verify that the derivative of $\tilde{f}_0$ is positive for all $\widetilde{x} = \alpha\tilde{\theta}_1$ with $\alpha \in [1/2, 1]$. This follows from assumption A6 and the expression of the derivative. Then, since $d\tilde{f}_0/d\widetilde{x} = 0$ at the extrema, the conclusion of the Lemma follows.

To further simplify the system, for large Hill coefficient m (assumption A2), the expression $V_2 x^m/(x^m + \theta_2^m)$ can be approximated by a step function with $s(x) = 0$ if $x < \theta_2$ and $s(x) = V_2$ if $x > \theta_2$. The expression $V_1 x^n/(x^n + \theta_1^n)$

can be aproximated by a piecewise linear function, so that the first nonlinear term $\Phi(x)$ in (3) can then be approximated by a continuous, piecewise linear or quadratic function, with three regions from now on labeled Φ^l (left), Φ^c (center) and Φ^r (right):

$$\begin{aligned}
\Phi^l(\widetilde{x}) &= \Phi_0(1-\widetilde{x}), && \widetilde{x} < (1-\Delta)\tilde{\theta}_1 \\
\Phi^c(\widetilde{x}) &= \left(\Phi_0 + \tfrac{V_1}{2\Delta\tilde{\theta}_1}(\widetilde{x} - (1-\Delta)\tilde{\theta}_1)\right)(1-\widetilde{x}), \\
& && (1-\Delta)\tilde{\theta}_1 \le \widetilde{x} \le (1+\Delta)\tilde{\theta}_1 \\
\Phi^r(\widetilde{x}) &= (\Phi_0 + V_1)(1-\widetilde{x}), && \widetilde{x} > (1+\Delta)\tilde{\theta}_1.
\end{aligned} \tag{4}$$

with $\Delta = 2/n$ and $1-\Delta = \frac{n-2}{n}$. Taking $\alpha = 1-\Delta$ in Lemma 4.1, we conclude that system (1) has a limit cycle whenever $\tilde{\theta}_2 \in [(1-\Delta)\tilde{\theta}_1, \tilde{\theta}_1]$.

V. Period of limit cycle

Assume now that conditions A1-A6 are satisfied, and system (1) has a limit cycle. The partial state $\widetilde{y}$ (genetic variable) represents a variable whose evolution is slow relative to $\widetilde{x}$ (signaling variable). Fig. 4 shows a decomposition of the cycle into four portions $(AB; BC; CD; DA)$. Portions BC and DA correspond to the jump of the protein x between a state of high concentration to a state of low concentration. Under the assumptions, the time spent by the trajectory on the portions BC and DA is much smaller than the time spent on the portions AB and CD [7]. The period of the limit cycle may then be approximated by the time to travel AB (T_1) and CD (T_2). From now on, for simplicity of notation, we will drop the tilde from variables x and y. In the nullcline $y = \tilde{f}_0(x)$, between the portion AB and CD, the second equation becomes

$$\frac{dy}{dt} \approx \tilde{f}_0'(x)\frac{dx}{dt} = \gamma_2\left(\frac{x^m}{x^m + \theta_2^m} - \tilde{f}_0(x)\right).$$

In the portion AB, approximating $\frac{x^m}{x^m+\theta_2^m}$ by a step function, we obtain the following equation:

$$\tilde{f}_0'(x)\frac{dx}{dt} = -\gamma_2\tilde{f}_0(x) \Rightarrow \int_{x_A}^{x_B}\frac{\tilde{f}_0'(x)}{\tilde{f}_0(x)}\,dx = -\int_0^{T_1}\gamma_2 dt$$

Integration gives:

$$T_1 = \frac{\ln\tilde{f}_0(x_A) - \ln\tilde{f}_0(x_B)}{\gamma_2}.$$

In the portion CD, with $G(x) = 1 - \tilde{f}_0(x)$,

$$\tilde{f}_0'(x)\frac{dx}{dt} = \gamma_2 G(x) \Rightarrow \int_{x_C}^{x_D}\frac{\tilde{f}_0'(x)}{G(x)}\,dx = \int_0^{T_2}\gamma_2 dt$$

and integration gives:

$$T_2 = \frac{\ln G(x_C) - \ln G(x_D)}{\gamma_2}.$$

Fig. 4 shows that $x_{\min} \approx x_B$, $x_{\max} \approx x_D$, $\tilde{f}_0(x_A) \approx \tilde{f}_0(x_D) \approx \tilde{f}_0(x_{\max})$ and that $\tilde{f}_0(x_C) \approx \tilde{f}_0(x_B) \approx \tilde{f}_0(x_{\min})$.

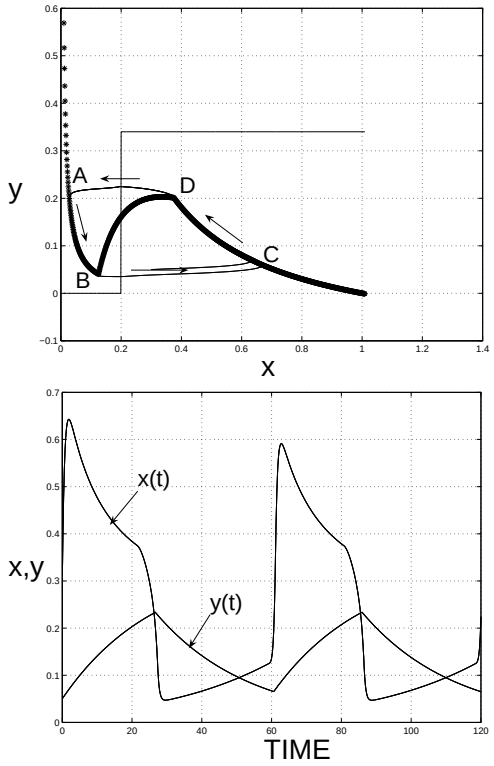

Fig. 4. Trajectories and limit cycle for the approximated fast/slow system. Top: the line marked $ABCDA$ represents the limit cycle. The bold (*) line represents the function $\tilde{f}_0(x)$, while the step function approximates $g_0(x)$ for large m. Bottom: trajectories of system (3), with $\Phi(x)$ approximated by (4) and $V_2x^m/(x^m+\theta_2^m)$ approximated by a step function. Parameters are as in Fig. 2.

Following Lemma 4.1, we approximate $x_{\min} \approx (1-\Delta)\theta_1$ and $x_{\max} \approx \theta_1$ to obtain (after algebraic simplification)

$$\begin{aligned}
\mathrm{P} \;\approx\; & \frac{1}{\gamma_2}\ln\left[\gamma_1\frac{V_2}{\Phi_0}\frac{(1-\Delta)\tilde{\theta}_1}{1-(1-\Delta)\tilde{\theta}_1} - \gamma_2\right] \\
& -\frac{1}{\gamma_2}\ln\left[\gamma_1\frac{V_2}{\Phi_0 + \frac{1}{2}V_1}\frac{\tilde{\theta}_1}{1-\tilde{\theta}_1} - \gamma_2\right].
\end{aligned} \tag{5}$$

For the example, in Fig. 4, the approximated period is 60s while the numerical full period is 56s, an error of 9% which could come from the approximations made for $x_{\min}$, $x_{\max}$, and $f_0(x)$. To guarantee that expression (5) is positive assume that:

$$\gamma_1 V_2\frac{1}{\Phi_0 + \frac{1}{2}V_1}\frac{\tilde{\theta}_1}{1-\tilde{\theta}_1} > 2\gamma_2 \tag{6}$$

$$\frac{1}{\Phi_0}\frac{(1-\Delta)\tilde{\theta}_1}{1-(1-\Delta)\tilde{\theta}_1} > \frac{1}{\Phi_0 + \frac{1}{2}V_1}\frac{\tilde{\theta}_1}{1-\tilde{\theta}_1}. \tag{7}$$

These conditions can be easily satisfied because, according to A1 we can choose γ_2 sufficiently small, and it also holds that $\Phi_0 \ll V_1$. By differentiating expression (5) relative to each parameter, it is observed that increasing V_1 or X_{tot} induces an increase in the period, while increasing Φ_0, θ_1, V_2 or γ_1 decreases the period. If we add the assumption

$\frac{1}{\Phi_0+\frac{1}{2}V_1}\frac{\tilde{\theta}_1}{1-\tilde{\theta}_1} > 1$, we verify that the period also decreases with γ_2 (see [8]). Some biological observations confirm these trends. For the biological system $p53$-Mdm2 [6], experiments show that an increase in Φ_0 reduces the period. For the system IκB-NFκB [4], one model [9] predicts a reduction of the period when V_2 increases.

VI. Parameter identification

As application of the regulation of a rapid signaling pathway by a slower process, we will use model (3) as a simple model for the mechanism of Cdc2 activation by cyclin B. This is is known to function as an autonomous oscillator [11] in the progression from G2 to M phases in the early embryonic cell cycle of *Xenopus* oocytes. Cyclin B (Φ_0) activates Cdc2 ($\widetilde{x}_0$) to form the complex Cdc2-cyclin B ($\widetilde{x}$). This complex activates its own activator, Cdc25 (the auto-feedback loop). At the same time, Cdc2 activates the Anaphase Promoting Complex (APC) ($\widetilde{y}$), which in turn promotes cyclin B degradation. The experiments reported in [11] can be interpreted as the response $\widetilde{x}$, to constant inputs Φ_0. The data consists of steady state values of $\widetilde{x}$, for each constant Φ_0. According to our analysis, if $\widetilde{x}$ is at steady state, then we expect *$\widetilde{y}$ to remain fixed at some (unknown) value $\widetilde{y}_0$*.

Under this hypothesis, model (3) can be reduced to the $\widetilde{x}$ equation, with a new parameter $\gamma_0 = \gamma_1\widetilde{y}_0$, to be estimated. The data in [11] can then in principle be used to estimate the parameters V_1, $\tilde{\theta}_1$, Δ and γ_0. In Fig. 6, the hysteresis curve for steady states of Cdc2-cyclin B as a function of the input Φ_0 (Fig. 3(c) of [11]) is reproduced as white squares and black stars. Note that the input term is, in general, of the form $\Phi_0 = k(u+u_b)$, where $u = [\delta 65 - \text{cyclin B}]$ represents the concentration of a special form of cyclin B (known input), u_b represents a basal concentration of cyclin B (unknown parameter), and k is the corresponding reaction rate, another parameter to be estimated.

From the piecewise quadratic expression (4), explicit analytic expressions for steady states as functions of the input u can be obtained. Analysis of (3) in Section III shows that there is a region of parameter Φ_0 where the system is bistable, i.e., it has two stable steady states (x^*_{low} and x^*_{high}) and one unstable steady state (x^*_{med}). In terms of the parameter u, this region will be denoted $[u_{\min}, u_{\max}]$. It is not difficult to check that the line $\psi = \gamma_0\widetilde{x}$ intersects Φ^l at most once, and Φ^c either once or twice (see also Fig. 5). In the latter case, $\psi = \gamma_0\widetilde{x}$ does not intersect Φ^r. In the former case, then $\psi = \gamma_0\widetilde{x}$ intersects each of the three pieces exactly once. Thus the two possible cases are:

$$
\begin{aligned}
x^a_{\text{low}} &= \frac{k(u+u_b)}{k(u+u_b)+\gamma_0} \quad \in [0,(1-\Delta)\tilde{\theta}_1)\\
x^a_{\text{med}} &= \frac{-c_1-\sqrt{c_1^2-4c_0c_2}}{2c_2} \ \in [1-\Delta,1+\Delta]\tilde{\theta}_1\\
x^a_{\text{high}} &= \frac{k(u+u_b)+V_1}{k(u+u_b)+V_1+\gamma_0} \quad \in ((1+\Delta)\tilde{\theta}_1,1],
\end{aligned}
$$

or

$$
\begin{aligned}
x^b_{\text{low}} &= \frac{k(u+u_b)}{k(u+u_b)+\gamma_0} \quad \in [0,(1-\Delta)\tilde{\theta}_1)\\
x^b_{\text{med}} &= \frac{-c_1-\sqrt{c_1^2-4c_0c_2}}{2c_2} \ \in [1-\Delta,1+\Delta]\tilde{\theta}_1\\
x^b_{\text{high}} &= \frac{-c_1+\sqrt{c_1^2-4c_0c_2}}{2c_2} \ \in [1-\Delta,1+\Delta]\tilde{\theta}_1,
\end{aligned}
$$

where

$$
\begin{aligned}
c_0 &= k(u+u_b) - \frac{V_1}{2}\frac{1-\Delta}{\Delta},\\
c_1 &= \frac{V_1}{2\Delta\tilde{\theta}_1}(1+(1-\Delta)\tilde{\theta}_1) - (ku+u_b) - \gamma_0,\\
c_2 &= -\frac{V_1}{2\Delta\tilde{\theta}_1}.
\end{aligned}
$$

In all experiments, measurements are given in terms of phosphoimager units, so the issue of converting these into concentration units should be considered. Since the total concentration X_{tot} is not known we will normalize data to the maximal steady state, and also normalize the mathematical equation to the theoretical steady state. To estimate the bistable region from the hysteresis data in Fig. 6, observe that $u_{\max}$ is the value for which the lower steady state coincides with $(1-\Delta)\theta_1$ (see Fig. 5, solid line):

$$
(1-\Delta)\tilde{\theta}_1 = x^*_{\text{low}} = \frac{k(u_{\max}+u_b)}{k(u_{\max}+u_b)+\gamma_0}
$$

yielding

$$
u_{\max} = -u_b + \frac{(1-\Delta)\tilde{\theta}_1}{1-(1-\Delta)\tilde{\theta}_1}\,\frac{\gamma_0}{k}.
$$

For the other extremity of the bistability interval, $u_{\min}$, there are two possible cases: either (i) $x^a_{\text{high}} = (1+\Delta)\tilde{\theta}_1$ or (ii) $x^b_{\text{med}} = x^b_{\text{high}}$. To see which of these two cases applies, note that for case (ii) $x^b_{\text{high}} = -c_1/(2c_2) \in [1-\Delta,1+\Delta]\tilde{\theta}_1$. If this condition is not valid, then case (ii) is not possible, and case (i) applies. The value of $u_{\min}$ can be computed by solving $c_1^2 = 4c_0c_2$ with respect to u, and then checking if it is in the required interval. For case (i), we have

$$
\begin{aligned}
(1+\Delta)\tilde{\theta}_1 &= \frac{k(u_{\min}+u_b)+V_1}{k(u_{\min}+u_b)+V_1+\gamma_0}\\
\Rightarrow \quad u_{\min} &= -u_b - \frac{V_1}{k} + \frac{(1+\Delta)\tilde{\theta}_1}{1-(1+\Delta)\tilde{\theta}_1}\,\frac{\gamma_0}{k}.
\end{aligned}
$$

(Note that the final result is as in case (ii), see Fig. 5, dash-dotted line.) These analytical expressions were compared to the data from the various experiments, and parameters estimated using a non-linear least squares method (in this case, the function `nonlinsq` from Matlab) to minimize:

$$
J_{ss}(V_1,\gamma_0,\tilde{\theta}_1,\Delta,u_b,k) = \sum_{u\in U}\left|\frac{\frac{x^*(u)}{x^*(100)}-\frac{w^*_u}{w^*_{100}}}{\frac{w^*_u}{w^*_{100}}}\right|^2
$$

$$
J_{bi}(V_1,\gamma_0,\tilde{\theta}_1,\Delta,u_b,k) = \sum_{i=\min,\max}\left|\frac{u_i-u_{obs,i}}{u_{obs,i}}\right|^2
$$

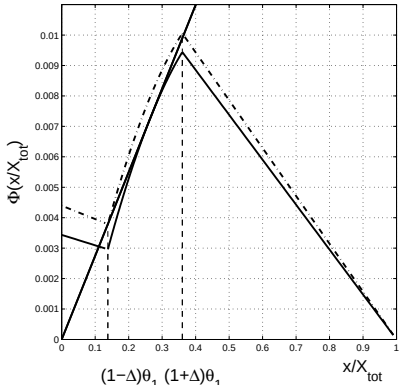

Fig. 5. The line $\gamma_0 \widetilde{x}$ and the piecewise quadratic function Φ, for the parameters of Table I and $u_{\min}$ (solid), $u_{\max}$ (dash-dot).

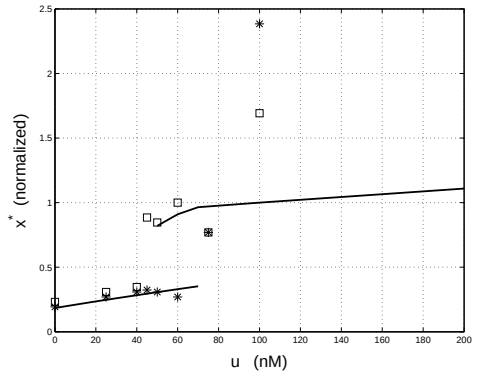

Fig. 6. Steady state response of the model (solid lines, parameters as in Table I). The stars and squares represent the hysteresis data in Fig. 3(c) of [11]. Note: the upper points at $u = 100$nM were not considered for the optimization process.

where $U = [0, 25, 40, 45, 50, 60, 75]$, and w_u^*, $u_{obs,i}$ denote the data points. To find a reasonable initial condition, we first computed the costs J_{ss} and J_{bi} on a grid ($V_1, \gamma_0 \in [0.005, 0.2]$, $\tilde{\theta}_1, \Delta \in [0.1, 0.9]$, $k = [10^{-5}, 10^{-4}]$, $u_b \in [10, 50]$), and then refined the grid based on the lower costs. Then choosing initial conditions on:

$$
\begin{aligned}
V_1 &\in \{0.008, 0.009, 0.01, 0.02\}, \\
\gamma_0 &\in \{0.015, 0.02, 0.025, 0.03\}, \\
\tilde{\theta}_1 &\in \{0.2, 0.25, 0.3, 0.35\}, \\
u_b &\in \{20, 25, 30, 35\}
\end{aligned}
$$

and running the optimization function for each point of this grid, the average results are shown in Table I.

Suppose now that the slower process governing y is added to the system. Choosing parameters V_2, γ_2 that satisfy assumptions A1-A6 the full system will exhibit a limit cycle.

TABLE I

ESTIMATED PARAMETERS.

Parameter	Value
V_1	0.01 s^{-1}
γ_0	0.028 s^{-1}
$\tilde{\theta}_1$	0.25
Δ	0.45
k	3.1×10^{-5} s^{-1}
u_b	66.7 nM
$u_{\min}$	45.9 nM
$u_{\max}$	77.3 nM

VII. CONCLUSIONS

The interaction between two pathways with different timescales was studied by coupling a one-element genetic network with a signal transduction pathway. A mechanism was proposed through which slowly varying gene expression patterns can induce rapid changes in the mode of operation of signal transduction networks, and also lead to sustained oscillations. From experimental data on the Cdc2-cyclin B system, parameters were identified. The obtained parameters satisfy the modeling assumptions, indicating that the mechanism coupling fast and slow dynamics is reasonable. The present analysis provides conditions for oscillatory behavior regulated by gene expression patterns, as well as estimates for the period of oscillations and its dependence on the model's parameters. Our results also suggest possible experiments to test the contribution of the negative feedback loop to the Cdc2-cyclin B dynamics, for instance, by identifying a suitable candidate for component y based on its activation threshold $\theta_2 \in [(1-\Delta), 1]\theta_1$.

VIII. ACKNOWLEDGEMENTS

This work was supported in part by the French Agence Nationale de la Recherche through the Biosys project MetaGenoReg.

REFERENCES

[1] U. Bhalla, P.T. Ram, and R. Iyengar. MAP kinase phosphatase as a locus of flexibility in mitogen-activated protein kinase signaling network. *Science*, 297:1018–1023, 2002.

[2] J.E. Ferrell and W. Xiong. Bistability in cell signalling: how to make continuous processes discontinuous, and reversible processes irreversible. *Chaos*, 11:227–238, 2001.

[3] R. Heinrich, B.G. Neel, and T.A. Rapoport. Mathematical models of protein kinase signal transduction. *Molecular Cell*, 9:957–970, 2002.

[4] A. Hoffmann, A. Levchenko, M.L. Scott, and D. Baltimore. The IkB-NFkB signaling module: temporal control and selective gene activation. *Science*, 298:1241–1245, 2002.

[5] B. N. Kholodenko. Negative feedback and ultrasensitivity can bring about oscillations in the mitogen-activated protein kinase cascades. *Eur. J. Biochem.*, 267:1583–1588, 2000.

[6] G. Lahav, N. Rosenfeld, A. Sigal, N. Geva-Zatorsky, A.J. Levine, M. Elowitz, and U. Alon. Dynamics of the p53-Mdm2 feedback loop in individual cells. *Nat. Genetics*, 36:147–150, 2004.

[7] J.D. Murray. *Mathematical Biology, 2nd edition*. Springer, Berlin, 2003.

[8] I. Ndiaye, M. Chaves, and J.-L. Gouzé. Un petit modèle d'interaction entre expression génétique et signalisation. In *Réseaux d'interactions : analyse, modélisation et simulation (RIAMS 07)*, Integrative Post-Genomics, Lyon, France, 2007.

[9] D.E. Nelson *et. al.* Oscillations in NF-κB signaling control the dynamics of gene expression. *Science*, 306:704–708, 2004.

[10] J.R. Pomerening, S.Y. Kim, and J.E. Ferrell. Systems-level dissection of the cell-cycle oscillator: bypassing positive feedback produces damped oscillations. *Cell*, 122:565–578, 2005.

[11] J.R. Pomerening, E.D. Sontag, and J.E. Ferrell. Building a cell cycle oscillator: hysteresis and bistability in the activation of Cdc2. *Nat. Cell Biol.*, 5:346–351, 2003.